Targeted imaging of urothelium carcinoma in human bladders by an ICG pHLIP peptide ex vivo

Jovana Golijanin[a,b], Ali Amin[c], Anna Moshnikova[b], Joseph M. Brito[a], Timothy Y. Tran[a], Ramona-Cosmina Adochite[b], Gregory O. Andreev[b], Troy Crawford[b], Donald M. Engelman[d,1], Oleg A. Andreev[b], Yana K. Reshetnyak[b,1], and Dragan Golijanin[a,1]

[a]Minimally Invasive Urology Institute, Division of Urology, The Miriam Hospital and The Warren Alpert Medical School of Brown University, Providence, RI 02906; [b]Physics Department, University of Rhode Island, Kingston, RI 02881; [c]Department of Pathology & Laboratory Medicine, Brown University, The Miriam Hospital, Providence, RI 02906; and [d]Department of Molecular Biophysics and Biochemistry, Yale University, New Haven, CT 06511

Edited by Owen N. Witte, Howard Hughes Medical Institute, University of California, Los Angeles, CA, and approved July 20, 2016 (received for review June 29, 2016)

Bladder cancer is the fifth most common in incidence and one of the most expensive cancers to treat. Early detection greatly improves the chances of survival and bladder preservation. The pH low insertion peptide (pHLIP) conjugated with a near-infrared fluorescent dye [indocyanine green (ICG)] targets low extracellular pH, allowing visualization of malignant lesions in human bladder carcinoma ex vivo. Cystectomy specimens obtained after radical surgery were immediately irrigated with nonbuffered saline and instilled with a solution of the ICG pHLIP construct, incubated, and rinsed. Bladders were subsequently opened and imaged, the fluorescent spots were marked, and a standard pathological analysis was carried out to establish the correlation between ICG pHLIP imaging and white light pathological assessment. Accurate targeting of bladder lesions was achieved with a sensitivity of 97%. Specificity is 100%, but reduced to 80% if targeting of necrotic tissue from previous transurethral resections or chemotherapy are considered as false positives. The ICG pHLIP imaging agent marked high-grade urothelial carcinomas, both muscle invasive and nonmuscle invasive. Carcinoma in situ was accurately diagnosed in 11 cases, whereas only four cases were seen using white light, so imaging with the ICG pHLIP peptide offers improved early diagnosis of bladder cancers and may also enable new treatment alternatives.

bladder cancer | fluorescence-guided surgery | NIR imaging | acidity | human tissue

Bladder cancer is the fifth most common cancer, constituting 4.5% of all new cancer cases in the United States; 76,960 new cases were estimated in 2016, and the death rate currently expected from bladder cancer is 21% (16,390). Approximately 2.4% of men and women will be diagnosed with bladder cancer at some point during their lifetime. In 2012, there were an estimated 577,403 individuals living with bladder cancer in the United States. Almost all of these patients require continuous surveillance, and occasionally, treatments. For all stages combined, the 5-y relative survival rate is 77%. Survival declines to 70% at 10 y and 65% at 15 y after diagnosis. Bladder cancer can be nonmuscle or muscle invasive. Half of all bladder cancer patients are diagnosed while the tumor is nonmuscle invasive, for which the 5-y survival is 96%. Most (up to 98%) of malignant bladder tumors arise in the epithelium; 90–92% of these bladder cancers are urothelial carcinomas (1, 2). Less common bladder cancers are squamous cell or adenocarcinomas. Approximately 20–25% of patients have muscle-invasive disease, and of non–muscle-invasive disease, patients will progress to muscle invasive disease at 5-y follow-up depending on intermediate or high risk of the progression (3, 4). An important medical objective is the identification of early stage lesions, such as carcinoma in situ, because it is expected that diagnosis at this stage will decrease the frequency of treatments, increasing patient health and reducing expense.

Each type and stage of bladder cancer requires a different type of treatment. High recurrence frequency, procedural costs, and the requirement for prolonged active monitoring make bladder cancer one of the most expensive cancers in the United States, placing a heavy economic burden on the health care system from lifetime endoscopic follow-ups and treatments. Patients suffer from high morbidity and the complications associated with chemotherapy, radiation, and radical surgery (5). Therefore, as noted, timely diagnosis of the tumor and appropriate management protocols are of great significance for decreasing treatment cost and improving a patient's lifestyle. Advances in the early detection of bladder cancer lesions are likely to increase the chances of timely successful treatment, the prevention of recurrences, and bladder function preservation.

Cancers, including urothelial carcinoma, are associated with multiple alterations in the genome, including changes in epigenetic regulation, point mutations, gene deletions, duplications, and chromosomal rearrangements. These changes are heterogeneous, leading to heterogeneity of the overexpression of particular biomarkers at the surfaces of cancer cells within a tumor and between tumors. Heterogeneity significantly limits success in the use of cell surface biomarkers for the targeted delivery of therapeutics. On other hand, multiple studies have revealed that neoplastic cells produce an acidic environment due to increased metabolic activity (6). Adaptations to the highly acidic microenvironment are critical steps in the transition from an avascular

Significance

Bladder cancer is the fifth most common cancer. Timely diagnosis and appropriate early management protocols are of paramount significance for improving patient outcomes. This study shows efficient pH-dependent near-infrared imaging of bladder malignant tumors without targeting of normal tissue. Our results demonstrate that the indocyanine green pH low insertion peptide (pHLIP) construct is suitable for use as a predictive clinical marker, specifically staining human bladder tumors after intravesical administration ex vivo. The targeting allows delivery of various imaging probes, which may offer early diagnosis and improve the outcomes of endoscopic and radical surgical resection of urothelial carcinomas. In addition, delivery of therapeutic molecules to cancer cells by pHLIP might open an opportunity for novel targeted treatment of bladder cancers.

Author contributions: A.A., O.A.A., Y.K.R., and D.G. designed research; J.G., A.A., A.M., J.M.B., T.Y.T., R.-C.A., T.C., and D.G. performed research; J.G., A.A., G.O.A., O.A.A., Y.K.R., and D.G. analyzed data; and A.A., D.M.E., O.A.A., Y.K.R., and D.G. wrote the paper.

Conflict of interest statement: Y.K.R., O.A.A., and D.M.E. are founders of a new company, pHLIP Inc. They have shares in the company, but the company did not fund any part of the work reported in the paper, which was done in their academic laboratories.

This article is a PNAS Direct Submission.

Freely available online through the PNAS open access option.

[1]To whom correspondence may be addressed. Email: dgolijanin@lifespan.org, reshetnyak@uri.edu, or donald.engelman@yale.edu.

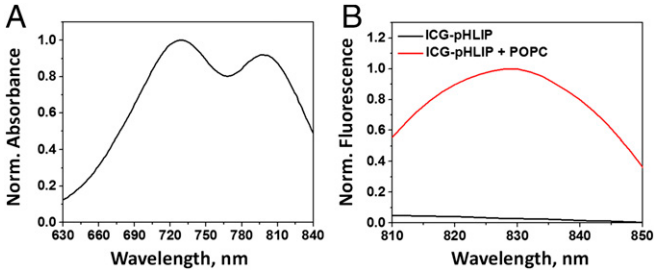

Fig. 1. Normalized absorbance (*A*) and fluorescence (*B*) spectra are shown of the ICG pHLIP construct measured in PBS, pH 7.4, containing 10 mM D-glucose. The fluorescence (with an excitation wavelength of 790 nm) of the ICG pHLIP construct is increased about 25-fold in the presence of POPC liposomes compared with the emission in buffer.

preinvasive tumor to a malignant invasive carcinoma (7–9). Thus, acidity may provide a universal biomarker for tumor targeting that is not subject to the selection of resistant cell lines (10). pH low insertion peptides (pHLIPs) are a class of membrane-binding peptides that specifically target acidic cells in vitro and in vivo (11) by inserting across cellular membranes when the extracellular pH is low (12). pHLIPs conjugated with fluorescent dyes have been used to differentiate normal from neoplastic tissue in various animal tumor models (12–15) and in human biopsy head and neck samples (16, 17). This report uses an indocyanine green (ICG) pHLIP conjugate for the diagnosis of urothelial carcinoma and precancerous lesions in fresh human radical cystectomy samples ex vivo and points the way toward a wide range of diagnostic and therapeutic alternatives.

Results

We used a pHLIP labeled with a near-infrared fluorescence (NIRF) dye, ICG, to monitor the targeting of tumors in human bladders. The absorption spectrum of ICG pHLIP is shown in Fig. 1*A*. The fluorescence of ICG pHLIP increases about 25-fold in the presence of 1-palmitoyl-2-oleoyl-sn-glycero-3-phosphocholine (POPC) liposomes (Fig. 1*B*). Thus, binding of ICG pHLIP to the lipid bilayers of cancerous cell membranes significantly enhances the emission of ICG.

From November 2014 through December 2015, 22 radical cystectomy patients were included in the study. Patient ages ranged from 51 to 84 y (mean age, 67.7 y), and the sex ratio of M/F was 19/3. Table 1 contains patient demographics, preoperative diagnosis, clinical stage of the disease, and the results of imaging studies. The specimens did not show any adverse morphological findings after incubation with ICG pHLIP, and there was no evidence of damage or degenerative effect in the nontumoral tissue. The use of ICG pHLIP did not alter the pathological assessment of the radical cystectomy tissues. Overall, 29 malignant lesions were identified by pathology assessment of the 22 bladder specimens stained with ICG pHLIP (3 radical cystectomy cases were incubated ex vivo with ICG-Cys as negative controls). The frequencies of different pathologies in 29 lesions were as follows: high-grade muscle invasive urothelial carcinoma (HGI) (Fig. 2 *A*–*C*) in 12; high-grade nonmuscle invasive urothelial carcinoma (HGN) (Fig. 2 *D*–*F*) in 5; carcinoma in situ (CIS) in 11 (Fig. 2 *G*–*I*), and high-grade dysplasia in 1 (Fig. 2 *J*–*L*). In seven cases, NIRF imaging guided the pathologist to CIS not observed by white light inspection. In case 2, necrotic tissue inside a diverticulum was NIRF positive. For the negative control cases (cases 13, 19, and 20) only the ICG-Cys dye alone was used for instillation (at concentrations from 8 to 40 μM in an 80-mL volume), and no specific tumor targeting was observed.

The tabular results of the sensitivity/specificity tests are shown in Tables 2–5. The test was performed for cancerous vs. normal tissue excluding targeting of necrotic and previously treated tissue (Tables 2 and 3). The sensitivity and specificity of targeting of cancerous tissue vs. normal were found to be 97% and 100%, respectively. If targeting of necrotic tissue from prior post transurethral removal of bladder tumors and previously treated (chemotherapy) necrotic tumors by ICG pHLIP is considered as a false positive, the specificity is reduced from 100% to 80% (Tables 4 and 5).

Discussion

We used an ICG pHLIP construct to target urothelial carcinoma in human bladder specimens immediately after surgical removal. ICG is a US Food and Drug Administration (FDA)-approved NIRF dye that does not show any independent propensity for targeting neoplastic tissue as seen in renal cell carcinoma, mostly by perfusion and diffusion differences or neoplastic and normal tissue (washout). ICG is in clinical use to visualize vasculature or lymphatics (18–20). ICG has a low level of fluorescence in aqueous solution, whereas its emission increases on binding to hydrophobic pockets of proteins (such as albumin) or cellular membranes. Targeting by the pHLIP is based on low pH-triggered insertion into the lipid bilayers of cancer cell membranes. Thus, the pHLIP tethers the ICG to the membrane, enhancing ICG fluorescence by about 25-fold.

To avoid/minimize targeting of normal cells by the ICG pHLIP, the construct was instilled in pH 7.4 PBS supplemented with 10 mM D-glucose to promote the uptake of the ICG pHLIP by cancer cells. Glycolytic cancer cells exhibit high glucose uptake, which enhances acidification of the extracellular space in vitro and in vivo (21). Thus, our goal was to selectively promote increased acidity at cancer cell surfaces to enhance pHLIP insertion and targeting while not affecting normal cells with normal metabolism.

In our study, we had a mixture of different subtypes of urothelial carcinoma, as expected given that the disease had advanced to the point where the bladder had to be removed. Our cases included typical high-grade urothelial carcinoma but also had different variants with prominent squamous cell differentiation, micropapillary urothelial carcinoma, adenocarcinoma, and plasmacytoid morphology. It appears that the sensitivity (97%) and specificity (100%) of tumor targeting by ICG pHLIP is irrelevant to the subtype of tumor. Half of the cystectomy specimens in our study revealed evidence of necrosis and effects from prior treatments, and all revealed evidence of residual tumor (invasive or in situ) adjacent and associated with necrosis, which was targeted by the ICG pHLIP, possibly from entrapment or uptake of ICG by necrotic areas. Our previous studies did not show targeting of necrotic tissue by pHLIPs in animal tumor models (14). If targeting of necrotic and previously treated tissues are considered as false positives, the specificity is decreased to 80%, but no false positives were seen for unperturbed lesions.

One lesion gave a positive NIRF imaging signal in the presence of dysplasia, revealed by subsequent pathology analysis. Urothelial dysplasia is an incidental microscopic finding where urothelial cells show mild atypical features short of the diagnosis of carcinoma in situ. It is considered a precancerous process, and studies have shown that up to 19% of urothelial dysplasia cases develop urothelial carcinoma (22–24). Although precancerous, it is recommended that patients with dysplasia receive proper clinical follow-up for early detection of an imminent carcinoma. Dysplasia has not been clinically detectable, so the ICG pHLIP may be a useful marker for detection of high-grade dysplasia in urothelium, allowing early detection of precancerous lesions.

Bladder tissues are prone to inflammation and infection. Long-standing inflammation and severe infections can cause transformations in the mucosa-like cystitis cystica and cystitis glandularis that, due to high frequency, are considered normal

Table 1. Demographic information, pathological stage and diagnosis, lesions seen by white light, and fluorescence imaging

Case no.	Sex/age (y)	Pathological stage	Pathological diagnosis	Grade	Lesion number	White light diagnosis	Fluorescence imaging
1	M/63	pT3aN1	Infiltrating high-grade urothelial carcinoma, CIS and necrosis	HGI	1	+	+
2	M/61	pT0N0	Diverticulum with urothelial atypia and treatment effects			+	+
3	F/84	ypT3bN0	Invasive high-grade urothelial carcinoma	HGI	2	+	+
			Invasive high-grade urothelial carcinoma and necrosis	HGI	3	+	+
4	M/51	pT2aN1	Residual infiltrative high-grade urothelial carcinoma micropapillary features, dysplasia and necrosis	HGI	4	+	+
5	M/69	pTaN0	Noninvasive high-grade papillary carcinoma	HGN	5	+	+
6	M/65	pT1N0	Residual invasive high-grade urothelial carcinoma, CIS and necrosis	HGI	6	+	+
			CIS	CIS	7	+	+
			CIS	CIS	8	+	+
7	M/61	pT1N0	Focally invasive high-grade urothelial carcinoma, necrosis	HGI	9	+	+
8	M/79	pT1N0	Dysplasia	DIS	10	−	+
			Treatment effect and CCCG			−	+
9	M/74	pT0N0	CCCG			−	+
10	F/82	pT1N0	Noninvasive high-grade urothelial carcinoma	HGN	11	+	+
			Invasive high-grade urothelial carcinoma	HGI	12	+	−
			CIS	CIS	13	−	+
			CIS and CCCG	CIS	14	−	+
11	M/68	pTisN0	CIS and CCCG	CIS	15	+	+
			CIS	CIS	16	−	+
12	M/71	pTisN0	Noninvasive high-grade urothelial carcinoma	HGN	17	+	+
			Noninvasive high-grade urothelial carcinoma	HGN	18	+	+
			CIS	CIS	19	−	+
			CIS	CIS	20	−	+
13*	M/66	pT3N1	Invasive high-grade urothelial carcinoma			+	ICG-Cys
			Ulceration, necrosis, CCCG			+	
14	M/66	pT1N0	Noninvasive high-grade urothelial carcinoma	HGN	21	+	+
15	M/57	pT1N0	Invasive high-grade urothelial carcinoma	HGI	22	+	+
16	F/77	pTisN0	CIS with early invasion	CIS	23	+	+
			CIS with early invasion	CIS	24	−	+
17†	M/57	pT1bN0	Invasive high-grade urothelial carcinoma	HGI	25	+	+
			CIS with early invasion	CIS	26	+	+
			Necrosis and treatment effect			+	+
18†	M/72	pT3aN0	Invasive high-grade urothelial carcinoma, CIS	HGI	27	+	+
			Necrosis and treatment effect in diverticulum			+	−
19	M/64	pT2aN0	Invasive high-grade urothelial carcinoma, CIS, Necrosis and treatment effect			+	ICG-Cys
20	M/63	ypT0N0	CCCG and reactive changes in scar			+	ICG-Cys
21	M/74	pT3aN0	Invasive high-grade urothelial carcinoma in scar	HGI	28	+	+
			Necrosis			+	+
22†	M/66	ypT3aN0	Invasive high-grade urothelial carcinoma with neuroendocrine features	HGI	29	+	+

+, Lesion was detected by white light or fluorescence imaging; −, lesion was not detected by white light or fluorescence imaging.
*Forty micromolar of 80 mL construct was used for instillation.
†Four micromolar of 80 mL construct was used for instillation.

findings in the urothelium. In one case, an area with marked uptake of the ICG pHLIP showed cystitis cystica et glandularis with chronic inflammation without any evidence of dysplasia or malignancy. It is noteworthy that almost all 22 cystectomy specimens revealed some degree of cystitis cystica et glandularis somewhere in the specimen. Only two lesions revealed cystitis cystica without any other pathology: one lesion (case 9) showed a positive signal with the ICG pHLIP. When the instilled concentration of the ICG pHLIP was reduced to 4 μM, the cystitis cystica in the second case (case 18) was not stained. Reducing the concentration of the ICG pHLIP did not affect targeting of high-grade invasive carcinoma and CIS (case 17). We expect that optimizing the concentration and shortening the time of the ICG pHLIP instillation will allow a clear signal differentiation among inflamed, necrotic, and cancerous tissue.

In summary, the ICG pHLIP peptide is a promising tool for the early detection of urothelial carcinoma, regardless of subtype, with high sensitivity and specificity. The detection might be used for monitoring the state of disease and/or for marking lesions for surgical removal. Before the ICG pHLIP imaging agent enters clinical trials, toxicology and pharmacology studies will be carried out to establish a safety profile. The ICG pHLIP imaging agent is expected to improve diagnosis and resection of cancerous lesions in the bladder. As a result, the recurrence rate might be reduced, patient outcomes could be improved, and the cost of medical care for bladder cancer will be lowered. In addition, success with targeted imaging could lead to pHLIP delivery of therapeutic molecules to bladder tumor cells, creating an opportunity for targeted treatment of bladder cancers. Currently, we are testing novel pHLIP-based therapeutic agents, which

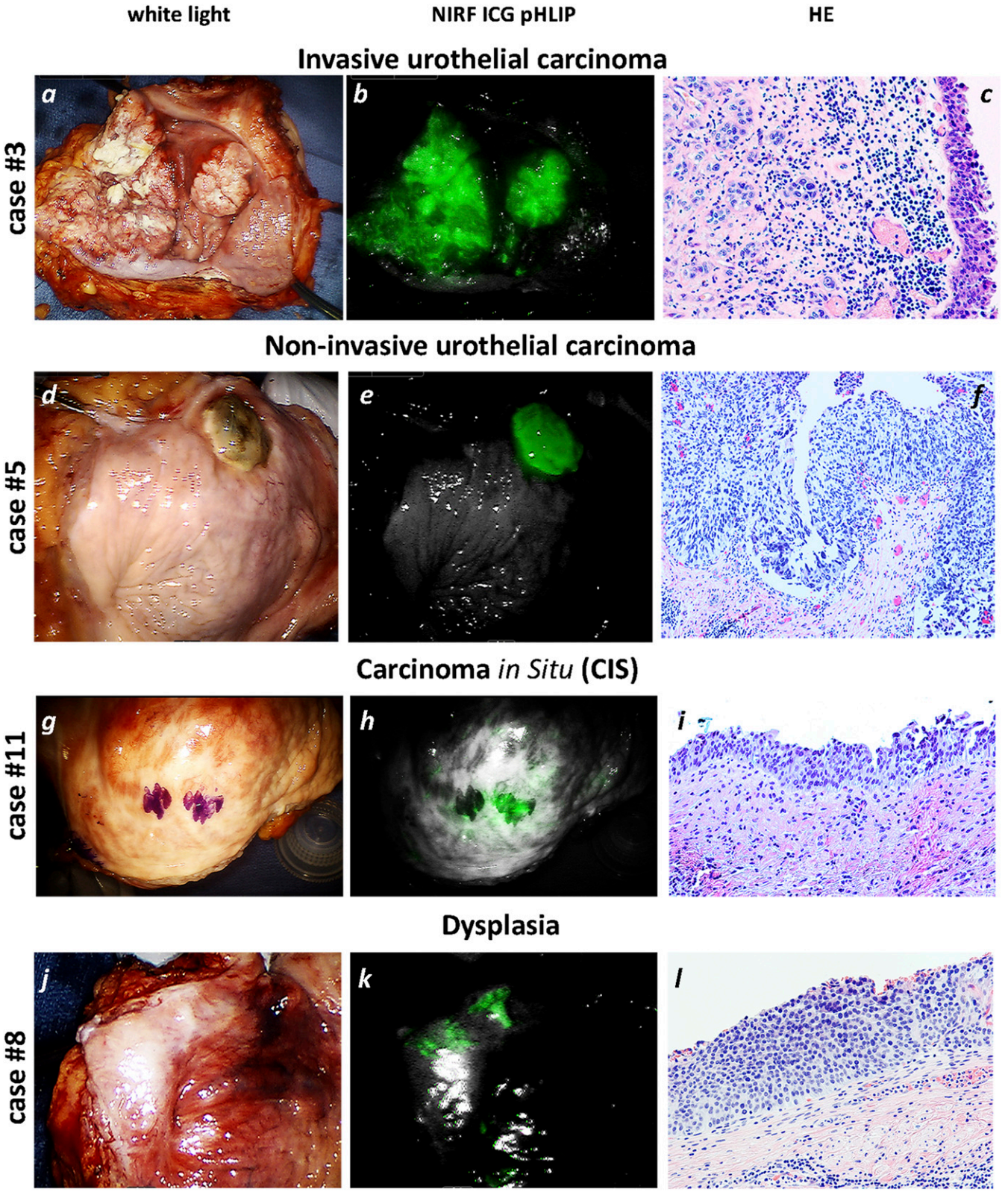

Fig. 2. Representative white light (*A*, *D*, *G*, and *J*), NIR fluorescence (*B*, *E*, *H*, and *K*) ex vivo imaging of bladder specimens and H&E stained tumor sections (*C*, *F*, *I*, and *L*) are shown, demonstrating targeting of invasive high-grade urothelial carcinoma (*A*–*C*), noninvasive high grade urothelial carcinoma (*D*–*F*), carcinoma in situ (*G*–*I*), and dysplasia (*J*–*L*) by the ICG pHLIP imaging agent. The diagnosis was confirmed by pathological analysis. The fluorescent lesions were marked in case 11 to identify locations for pathology analysis.

Table 2. Tabular results of the sensitivity/specificity test of ICG pHLIP peptide targeting of cancerous lesions in the human bladder specimens: carcinoma vs. normal excluding necrotic tissue and treatment effects

Receiver operator characteristics carcinoma vs. normal	*TP* + *FN*	*FP* + *TN*	Sum
TP + *FP*	*TP*, 28	*FP*, 0	28
FN + *TN*	*FN*, 1	*TN*, 19	20
Sum	29	19	

TP is the true positive; *TN* is the true negative; *FP* is the false positive; *FN* is the false negative.

Table 4. Tabular results of the sensitivity/specificity test of ICG pHLIP peptide targeting of cancerous lesions in the human bladder specimens: carcinoma vs. normal including necrotic tissue and treatment effects

Receiver operator characteristics carcinoma vs. normal + necrosis	*TP* + *FN*	*FP* + *TN*	Sum
TP + *FP*	*TP*, 28	*FP*, 5	33
FN + *TN*	*FN*, 1	*TN*, 20	21
Sum	29	25	

TP is the true positive; *TN* is the true negative; *FP* is the false positive; *FN* is the false negative.

demonstrate very promising results. Further, the ICG pHLIP construct is a generally applicable imaging agent, because it targets a general property of the tumor microenvironment, tumor acidity. Once approved for clinical use, it could be tested and possibly used on a variety of cancers. We have shown targeting of primary tumors and metastatic lesions by fluorescent pHLIPs in more than 15 varieties of human, murine, and rat tumors, including lymphoma, melanoma, pancreatic, breast, and prostate transgenic mouse models and human tissue (bladder, kidney, breast, and head/neck stained ex vivo).

Materials and Methods

Conjugation of ICG with the pHLIP Peptide. pHLIP variant 3 (Var3) peptide with a single Cys residue at the N terminus, ACDDQNPWRAYLDLLFPTDTLLLDLLWA, was synthesized and purified by reversed phase chromatography by CS Bio. The near infrared fluorescent dye, ICG maleimide (Intrace Medical), was conjugated to the pHLIP peptide at a ratio of 1:1 in dimethylformamide (DMF). The reaction progress was monitored by the reversed phase (Zorbax SB-C18 columns, 9.4 × 250 mm, 5 μm; Agilent Technology) HPLCy (HPLC) using a gradient from 5% to 70% acetonitrile in water containing 0.05% trifluoroacetic acid. Also, for the negative control, ICG-malemide was conjugated with the free amino acid, L-cysteine (Sigma). The concentration of labeled peptide in buffer was determined by ICG absorption at 800 nm, ε_{800} = 137,000 $M^{-1}{\cdot}cm^{-1}$. The purity of the constructs was performed by analytical HPLC and surface-enhanced laser desorption/ionization time-of-flight (SELDI-TOF) MS, and the amount of free dye in the solution was less than 1%.

Liposome Preparation. Large unilamellar vesicles were prepared by extrusion; 2.5 mg POPC (1-palmitoyl-2-oleoyl-snglycero-3-phosphocholine; Avanti Polar Lipids) lipids were dissolved in 0.5 mL chloroform, desolvated on a rotary evaporator, and dried under high vacuum for 3 h. The phospholipid film was then rehydrated in pH 7.4 PBS containing 10 mM D-glucose, vortexed for 5 min, and repeatedly extruded at least 15 times through a membrane with a 100-nm pore size.

Absorption and Fluorescence Measurements. Absorbance and fluorescence measurements were carried out on a Genesys 10S UV-Vis spectrophotometer (Thermo Scientific) and a SpectraMax M2 spectrofluorometer (Molecular Devices), respectively. The absorption spectra were measured in PBS, pH 7.4, containing 10 mM D-glucose from 600 to 850 nm. The fluorescence spectra of 10 μM of ICG pHLIP peptide were measured from 810 to 850 nm at 790-nm excitation wavelength in PBS, pH 7.4, containing 10 mM D-glucose, with or without 2 mM of POPC liposomes.

Ex Vivo Imaging of Bladder Specimens. After obtaining institutional review board approval from Rhode Island Hospital, Lifespan, 22 urothelial carcinoma patients that were scheduled for radical cystectomy were selected over a 12-mo period and appropriate informed consent was obtained. After radical cystectomy, bladder specimens were immediately removed and irrigated three times for 5 min via catheter with nonbuffered saline and instilled and incubated with 80 mL of 8 μM or 32.8 μg/mL (unless otherwise is stated, see notes to Table 1) of ICG pHLIP construct or ICG-Cys in PBS, pH 7.4, containing 10 mM D-glucose for 60 min. Then, the unbound constructs were removed by rinsing with 80 mL of saline solution three to five times, the bladder was irrigated thoroughly with buffered saline and opened using a Y incision on the anterior wall. Using a da Vinci Si NIRF imaging system (FireflyR), ex vivo fluorescent and white light imaging of the entire bladder and its parts was performed. The fluorescent spots were marked and standard pathological analysis was carried out to explore the correlation between appearance of fluorescent signal and cancer lesions.

Pathological Analysis. The specimen was sectioned and submitted after 24-h fixation in 10% phosphate-buffered formalin according to the standard institutional grossing manual, with emphasis on the marked areas of the bladder. The sections were processed for routine histology into paraffin-embedded blocks. Five-micrometer-thick tissue sections were obtained and stained for H&E. Evaluation of pathology was performed by a genitourinary pathologist, and a standard report was prepared based on the American Joint Committee on Cancer Cancer Staging Manual, seventh edition, 2010.

Statistical Analysis. Statistical parameters were calculated according to the following equations:

$$TRP = \frac{TP}{TP + FN}; \quad SPC = \frac{TN}{TN + FP},$$

$$PPV = \frac{TP}{TP + FP}; \quad NPV = \frac{TN}{FN + TN},$$

$$FPR = \frac{FP}{FP + TN}; \quad FNR = \frac{FN}{TP + FN},$$

$$FDR = \frac{FP}{TP + FP}; \quad FOR = \frac{FN}{FP + TN},$$

where *TP* is the true positive; *TN* is the true negative; *FP* is the false positive; *FN* is the false negative; *TRP* is the true positive rate or sensitivity; *SPC* is the true negative rate or specificity; *PPV* is the positive predictive value or precision; *NPV* is the negative predictive values; *FPR* is the false positive rate;

Table 3. Descriptive parameters

Measure	Results
Sensitivity, *TRP*	0.966
Specificity, *SPC*	1.000
Positive predictive value, *PPV*	1.000
Negative predictive values, *NPV*	0.950
False positive rate, *FPR*	0.000
False negative rate, *FNR*	0.034
False discovery rate, *FDR*	0.000
False omission rate, *FOR*	0.053

Table 5. Descriptive parameters

Measure	Results
Sensitivity, *TRP*	0.966
Specificity, *SPC*	0.800
Positive predictive value, *PPV*	0.848
Negative predictive values, *NPV*	0.952
False positive rate, *FPR*	0.020
False negative rate, *FNR*	0.034
False discovery rate, *FDR*	0.152
False omission rate, *FOR*	0.040

FNR is the false negative rate; *FDR* is the false discovery rate; and *FOR* is the false omission rate.

ACKNOWLEDGMENTS. This work was supported by NIH Grant GM073857 (to D.M.E., O.A.A., and Y.K.R.).

1. Siegel R, Naishadham D, Jemal A (2012) Cancer statistics, 2012. *CA Cancer J Clin* 62(1): 10–29.
2. Pasin E, Josephson DY, Mitra AP, Cote RJ, Stein JP (2008) Superficial bladder cancer: An update on etiology, molecular development, classification, and natural history. *Rev Urol* 10(1):31–43.
3. Anastasiadis A, de Reijke TM (2012) Best practice in the treatment of nonmuscle invasive bladder cancer. *Ther Adv Urol* 4(1):13–32.
4. Kamat AM, et al. (2014) Defining and treating the spectrum of intermediate risk nonmuscle invasive bladder cancer. *J Urol* 192(2):305–315.
5. Mariotto AB, Yabroff KR, Shao Y, Feuer EJ, Brown ML (2011) Projections of the cost of cancer care in the United States: 2010-2020. *J Natl Cancer Inst* 103(2):117–128.
6. Damaghi M, Wojtkowiak JW, Gillies RJ (2013) pH sensing and regulation in cancer. *Front Physiol* 4:370.
7. Gillies RJ, Verduzco D, Gatenby RA (2012) Evolutionary dynamics of carcinogenesis and why targeted therapy does not work. *Nat Rev Cancer* 12(7):487–493.
8. Estrella V, et al. (2013) Acidity generated by the tumor microenvironment drives local invasion. *Cancer Res* 73(5):1524–1535.
9. Gatenby RA, Gawlinski ET, Gmitro AF, Kaylor B, Gillies RJ (2006) Acid-mediated tumor invasion: A multidisciplinary study. *Cancer Res* 66(10):5216–5223.
10. Bailey KM, Wojtkowiak JW, Hashim AI, Gillies RJ (2012) Targeting the metabolic microenvironment of tumors. *Adv Pharmacol* 65:63–107.
11. Andreev OA, Engelman DM, Reshetnyak YK (2014) Targeting diseased tissues by pHLIP insertion at low cell surface pH. *Front Physiol* 5:97.
12. Weerakkody D, et al. (2013) Family of pH (low) insertion peptides for tumor targeting. *Proc Natl Acad Sci USA* 110(15):5834–5839.
13. Reshetnyak YK, et al. (2011) Measuring tumor aggressiveness and targeting metastatic lesions with fluorescent pHLIP. *Mol Imaging Biol* 13(6):1146–1156.
14. Adochite RC, et al. (2014) Targeting breast tumors with pH (low) insertion peptides. *Mol Pharm* 11(8):2896–2905.
15. Cruz-Monserrate Z, et al. (2014) Targeting pancreatic ductal adenocarcinoma acidic microenvironment. *Sci Rep* 4:4410.
16. Luo Z, et al. (2014) Widefield optical imaging of changes in uptake of glucose and tissue extracellular pH in head and neck cancer. *Cancer Prev Res (Phila)* 7(10): 1035–1044.
17. Luo Z, Tikekar RV, Samadzadeh KM, Nitin N (2012) Optical molecular imaging approach for rapid assessment of response of individual cancer cells to chemotherapy. *J Biomed Opt* 17(10):106006.
18. Tobis S, et al. (2012) Robot-assisted and laparoscopic partial nephrectomy with near infrared fluorescence imaging. *J Endourol* 26(7):797–802.
19. Alander JT, et al. (2012) A review of indocyanine green fluorescent imaging in surgery. *Int J Biomed Imaging* 2012:940585.
20. Desmettre T, Devoisselle JM, Mordon S (2000) Fluorescence properties and metabolic features of indocyanine green (ICG) as related to angiography. *Surv Ophthalmol* 45(1):15–27.
21. Kozin SV, Shkarin P, Gerweck LE (2001) The cell transmembrane pH gradient in tumors enhances cytotoxicity of specific weak acid chemotherapeutics. *Cancer Res* 61(12):4740–4743.
22. Althausen AF, Prout GR, Jr, Daly JJ (1976) Non-invasive papillary carcinoma of the bladder associated with carcinoma in situ. *J Urol* 116(5):575–580.
23. Smith G, et al. (1983) Prognostic significance of biopsy results of normal-looking mucosa in cases of superficial bladder cancer. *Br J Urol* 55(6):665–669.
24. Zuk RJ, Rogers HS, Martin JE, Baithun SI (1988) Clinicopathological importance of primary dysplasia of bladder. *J Clin Pathol* 41(12):1277–1280.